IEEE Photonics Journal
An IEEE Photonics Society Publication

Open Access

# Resonant Mode Characteristics of Microfiber Knot-Type Ring Resonator and Its Salinity Sensing Experiment

Volume 7, Number 4, August 2015

**Yipeng Liao**
**Xin Wang**
**Hongjuan Yang**
**Shanshan Wang**
**Jing Wang**

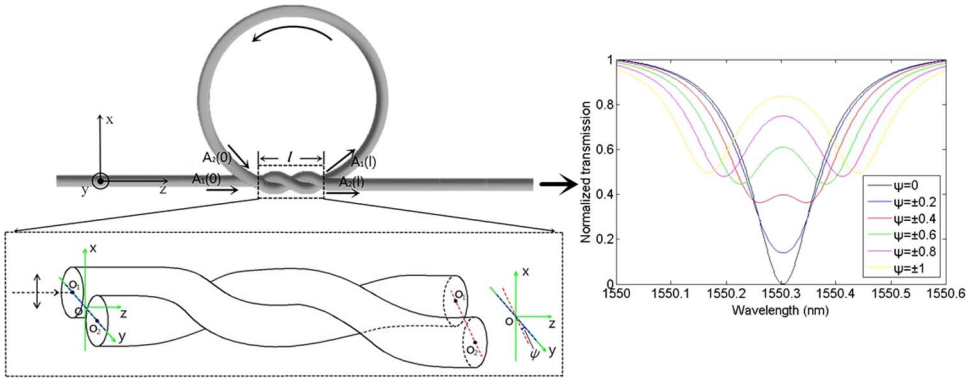


DOI: 10.1109/JPHOT.2015.2450533
1943-0655 

IEEE photonics SOCIETY

IEEE

# Resonant Mode Characteristics of Microfiber Knot-Type Ring Resonator and Its Salinity Sensing Experiment

**Yipeng Liao, Xin Wang, Hongjuan Yang, Shanshan Wang, and Jing Wang**

Laboratory of Optics and Optoelectronics, Department of Physics,
Ocean University of China, Qingdao 266100, China

*DOI: 10.1109/JPHOT.2015.2450533*


Manuscript received June 2, 2015; revised June 23, 2015; accepted June 23, 2015. Date of publication June 30, 2015; date of current version July 10, 2015. This work was supported by the Natural Science Foundation of China under Grant 61171161 and Grant 61405181. Corresponding author: J. Wang (e-mail: wjing@ouc.edu.cn).

**Abstract:** The microfiber knot-type ring resonator is widely used in sensing, and the resonant mode is an essential concern. In this paper, resonant mode characteristics of microfiber knot-type ring resonator are studied theoretically. Results show that resonant mode split occurs when the deviation angle is large enough under the condition that the input is linearly or elliptically polarized light. Moreover, in the case that the input is partially polarized light, the resonant peak positions of split modes are identical with those in the case of inputting linearly or elliptically polarized light under the same deviation angle. The split mode characteristic is further studied by salinity sensing simulation and experiment. The split modes have the same free spectral range, and their resonant peak shifts have the same response to salinity changing. The experimental split mode characteristic is in good agreement with theoretical simulating, which demonstrates the resonant mode split theory of the microfiber knot-type ring resonator. The analysis on resonant mode presented here may offer useful references for sensing applications.

**Index Terms:** Resonant mode, salinity sensing, knot-type ring resonator, twisted coupler.

## 1. Introduction

In recent years, fiber sensors have become a focus due to their advantages of high sensitivity, fast response, and electromagnetic immunity. Many fiber-based surface plasmon (SP) sensors have been successfully fabricated, such as the fiber-optic chemical sensor [1], the microstructured optical fiber-based surface plasmon resonance (MOF-based SPR) sensor [2], the tilted fiber Bragg grating-based surface plasmon resonance aptasensor [3], and the on-fiber plasmonic interferometer [4]. These sensors have great potential application in biochemical sensing. However, the fiber-based SPs sensors usually need a fine metal coating, special fibers and UV laser photolithograph to fabricate the tilted fiber Bragg grating and the microstructured fiber, which increases equipment cost and manufacturing difficulty. Compared to the above approaches, the microfiber knot-type ring resonator (MKR) is a new sensor with high sensitivity, simpler structure, smaller size and lower cost. Many efforts have been devoted to the study on various parameters sensing by utilizing MKR, such as refractive index [5], [6], temperature [7], [8], humidity [9], [10], electric current [11] and magnetic field [12]. The resonant-wavelength-shift scheme which depends on the relationship between resonant wavelength shifts and variation of

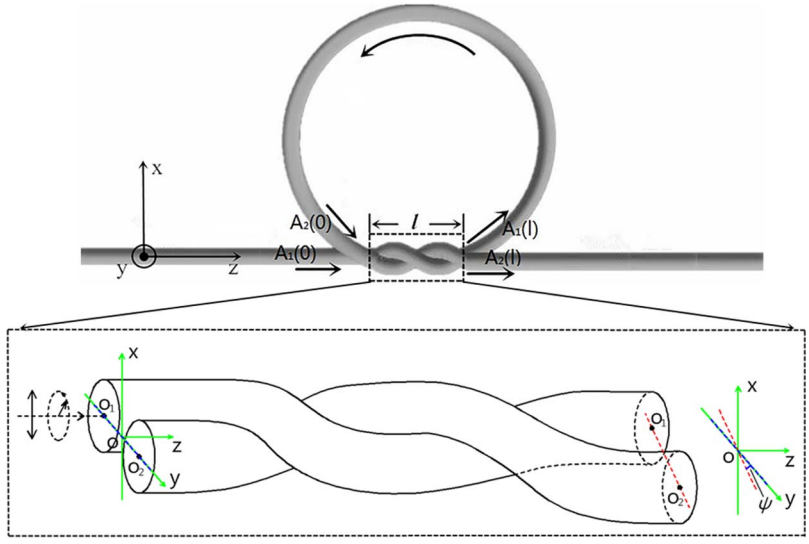


Fig. 1. Schematic diagram of MKR. The inset shows the knot area (twisted coupler).

ambient is used in most MKR-based sensing. Thus, it is important to analyze the resonant mode of MKR.

Currently, the study on MKR transmission characteristic and sensing by Yang *et al.* [5], [8], [10], [11] is still using the theory of microfiber loop resonator (MLR) [13], [14], which takes only one resonant mode into consideration. However, the transmission spectra with multiple resonant modes are obtained by Lim *et al.* [5], [10], which cannot be in agreement with the MLR theory. The effect of refined structure on transmission characteristic is taken into consideration these years. For instance, the polarization effect of MKR result from lack of circular symmetry is theoretically investigated by Wang [15]. Based on temporal coupled mode theory, mode splitting of coupled cavity system is analyzed by Li [16]. Yu's theoretical results show that knot area structure greatly affects the resonant mode [17]; however, the theory is established in the case of inputting linearly polarized light and do not consider that the broadband light in experiment usually is partially polarized light. Moreover, there is lack of experimental verification of the theory. In short, the effect of refined structure on transmission characteristic has not been systematically considered and thus a more detailed analysis of resonant mode is needed to improve the theory of MKR.

In this paper, we theoretically investigate the relationship between deviation angle of knot area and resonant mode split in the case of inputting linearly, elliptically and circularly polarized light. Considering that partially polarized light is usually used as the input in experiment, resonant mode split in the case of inputting partially polarized light is also studied. In addition, the characteristic of split modes are further studied in salinity sensing simulation. To verify the resonant mode split theory of MKR, salinity sensing experiment is performed. Results presented here may offer useful references for MKR-based sensing applications.

## 2. Theoretical Analyses

### 2.1. Fundamental Theory of MKR

The schematic model of a MKR is shown in Fig. 1. The input light is divided into two parts after passing the twisted coupler, one of that outputs through the output port directly, the other one goes back to the twisted coupler after passing the microfiber ring. Likewise, the light going back to the twisted coupler is also divided into two parts, which transfer to the output port and microfiber ring, respectively. Finally, a stable light field is formed after the above process is repeated.

The light field can be decomposed into x-direction and y-direction components and expressed as $A = [a_x, a_y]$. The effect of twisted coupler on the input light field can be characterized by the coupled mode equation [18], the relationship among light fields in four ports can be expressed as

$$\begin{bmatrix} a_{1x'}(l) \\ a_{1y'}(l) \\ a_{2x'}(l) \\ a_{2y'}(l) \end{bmatrix} = \begin{bmatrix} t_{11} & t_{12} & t_{13} & t_{14} \\ -t_{12} & t_{22} & -t_{14} & t_{24} \\ t_{13} & t_{14} & t_{11} & t_{12} \\ -t_{14} & t_{24} & -t_{12} & t_{22} \end{bmatrix} \cdot \begin{bmatrix} a_{1x}(0) \\ a_{1y}(0) \\ a_{2x}(0) \\ a_{2y}(0) \end{bmatrix} \exp(-i\beta l) \tag{1}$$

where $\beta$ is the propagation constant; $l$ is the length of the coupler region; matrix elements $t_{11}, t_{12}, t_{13}, t_{14}, t_{22},$ and $t_{24}$ are related to the twisting angle $\theta$, length of the coupler region $l$, and coupling coefficient; and they can be expressed as

$$\begin{aligned} t_{11} &= \cos C_0 l \cos C_a l - \cos\gamma \sin C_0 l \sin C_a l, & t_{12} &= \sin\gamma \sin C_0 l \cos C_a l \\ t_{13} &= -j(\cos C_0 l \sin C_a l + \cos\gamma \sin C_0 l \cos C_a l), & t_{14} &= -j \sin\gamma \sin C_0 l \sin C_a l \\ t_{22} &= \cos C_0 l \cos C_a l + \cos\gamma \sin C_0 l \sin C_a l, & t_{24} &= -j(\cos C_0 l \sin C_a l - \cos\gamma \sin C_0 l \cos C_a l) \end{aligned}$$

$$C_0 = \sqrt{C_b^2 + \sigma^2}, \quad \sin\gamma = \frac{\sigma}{\sqrt{C_b^2 + \sigma^2}}, \quad \cos\gamma = \frac{C_b}{\sqrt{C_b^2 + \sigma^2}}, \quad \theta = \sigma l.$$

As to the coupling between two uniform fibers, the coupling coefficient is $C_a$, and $C_b = 0$.

There is a phase delay between $A_2(0)$ and $A_1(l)$, and thus, the transmission Jones matrix through the microfiber ring can be given by

$$\begin{bmatrix} a_{2x}(0) \\ a_{2y}(0) \end{bmatrix} = \alpha \exp(-i\beta L) \begin{bmatrix} a_{1x}(l) \\ a_{1y}(l) \end{bmatrix} \tag{2}$$

where $\alpha$ is the total loss coefficient after a circular propagation, and $L$ is the length of the microfiber ring.

By jointly solving (1) and (2), the transmission equation of MKR can be obtained as

$$\begin{bmatrix} a_{2x}(l) \\ a_{2y}(l) \end{bmatrix} = T \cdot \begin{bmatrix} a_{1x}(0) \\ a_{1y}(0) \end{bmatrix} \tag{3}$$

where $T$ is the transmission matrix of the MKR

$$T = \begin{bmatrix} T_{11} & t_{12} \\ T_{21} & t_{22} \end{bmatrix} \tag{4}$$

where

$$\begin{aligned} T_{11} = T_{22} = &\left\{ (t_{13}^3 + t_{13}t_{12}^2 + t_{13}t_{14}^2 - t_{13}t_{11}^2)\exp(-2i\beta l) - 2t_{11}t_{12}t_{14}\exp(-i\beta l) \right. \\ &\left. - \frac{1}{\alpha}(t_{12}^2 + 2t_{13}^2 - t_{11}^2)\exp[i\beta(L-l)] + \frac{1}{\alpha^2} t_{13}\exp(2i\beta L) \right\} \\ &\cdot \left\{ \left[ t_{24}\exp(-i\beta l) - \frac{1}{\alpha}\exp(i\beta L) \right] \cdot \left[ t_{13}\exp(-i\beta l) - \frac{1}{\alpha}\exp(i\beta L) \right] + t_{14}^2\exp(-2i\beta l) \right\}^{-1} \\ T_{12} = -T_{21} = &\left\{ (t_{14}^3 + t_{14}t_{13}^2 - 2t_{11}t_{12}t_{13})\exp(-2i\beta l) + (t_{14}t_{11}^2 - t_{14}t_{12}^2)\exp(-i\beta l) \right. \\ &\left. + \frac{2}{\alpha}(t_{11}t_{12} - t_{13}t_{14})\exp[i\beta(L-l)] + \frac{1}{\alpha^2} t_{14}\exp(2i\beta L) \right\} \\ &\cdot \left\{ \left[ t_{24}\exp(-i\beta l) - \frac{1}{\alpha}\exp(i\beta L) \right] \cdot \left[ t_{13}\exp(-i\beta l) - \frac{1}{\alpha}\exp(i\beta L) \right] + t_{14}^2\exp(-2i\beta l) \right\}^{-1}. \end{aligned}$$

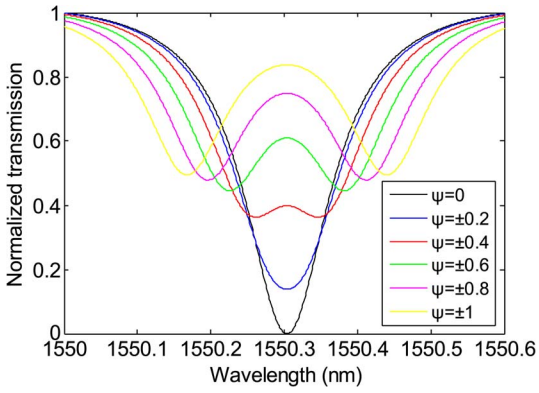


Fig. 2. Normalized transmission spectra in the case of inputting linearly polarized light.

Output light intensity can be expressed as

$$I = [\mathrm{A}_2(l)]^2 = [a_{2x}(l)]^2 + [a_{2y}(l)]^2 \tag{5}$$

depending on the deviation angle $\psi$ and the polarized state of incident light.

### 2.2. Relationship Between Resonant Mode Split and Deviation Angle

In this work, a MKR with 600-$\mu$m-diameter is designed to study the effect of polarized state and deviation angle on resonant mode split. Other parameters are set as follows: $l = 150$ $\mu$m, $\alpha = 0.98$, the coupling coefficient $C_a$ of the twisted coupler is 0.98, microfiber has a diameter of 3 $\mu$m, $\beta$ is determined by solving eigenvalue equation [19], [20]. The twisting angle $\theta$ is not exactly equal to $2\pi$ in many practical situation and can be written as $\theta = 2\pi + \psi$ (the angle values are in radian units in this paper); the deviation angle value $|\psi|$ is relatively large especially under the influence of tension in liquid.

Based on the model mentioned above, the dependence of resonant mode split on deviation angle $\psi$ in the case of inputting linearly polarized light is investigated. Fig. 2 shows the normalized transmission spectra when $\mathrm{A}_1(0) = [1, 0]$. The transmission spectra highly depend on the deviation angle value $|\psi|$, and resonant mode split occurs with the increasing $|\psi|$. The split modes symmetrically distributed on both sizes of resonant mode in the case of $\psi = 0$, and the spacing of split modes increases with the increasing $|\psi|$, the extinction ratios decrease with the increasing $|\psi|$.

Then, the dependence of resonant mode split on deviation angle $\psi$ in the case that the input is elliptically polarized light is investigated. Fig. 3. shows the normalized transmission spectra when $\mathrm{A}_1(0) = 5/\sqrt{26}[1, i/5]$. It is noticed that the increase of $\psi$ result in resonant mode split. The positions of split modes symmetrically distributed on both sizes of resonant mode in the case of $\psi = 0$, the spacing of split modes increase with the increasing $|\psi|$; however, the extinction ratios of split modes are different.

The dependence of resonant mode split on deviation angle $\psi$ in the case of inputting circularly polarized light is also investigated. When $\mathrm{A}_1(0) = 1\sqrt{2}[1, i]$, the normalized transmission spectra are shown in Fig. 4. Unlike previous situations, the increase of $\psi$ do not affect resonant mode split and the extinction ratio, but make the resonant peak shift.

As can be seen, the practical deviation angle $|\psi|$ of twisted coupler has a great influence on resonant mode split of MKR. In the case of inputting linearly and elliptically polarized light, the increase of $|\psi|$ result in resonant mode split. It can be explained as following: linearly and elliptically polarized light can be decomposed into left and right circularly polarized light. When light transfers to the twisted coupler, left and right circularly polarized light have different propagation constant. Hence, their resonances are mutually independent and then the synthetic spectra have two resonant modes. In particular, a single circularly polarized light has a certain propagation constant, so resonant mode split cannot be obtained.

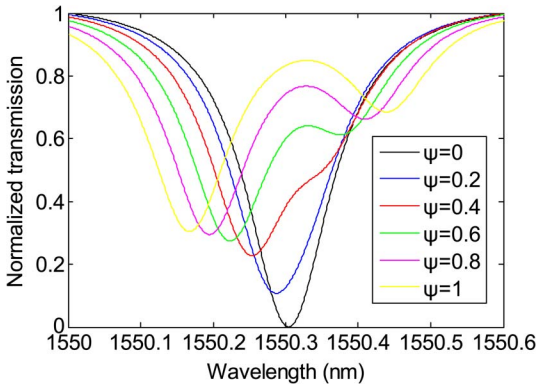


Fig. 3. Normalized transmission spectra in the case of inputting elliptically polarized light.

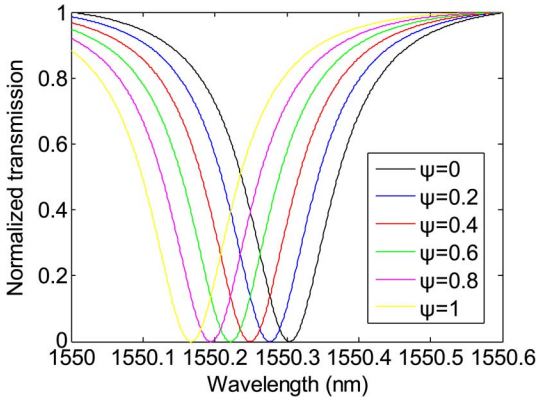


Fig. 4. Normalized transmission spectra in the case of inputting circularly polarized light.

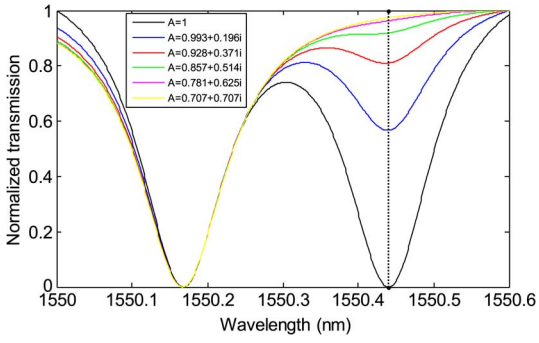


Fig. 5. Normalized transmission spectra in the case of inputting light with different polarization states.

### 2.3. Characteristics of Split Modes

Below, the split modes are investigated on the condition that the input light has different polarized states and that MKRs have the same $\psi$. Based on the model mentioned in Section 2.2, deviation angles are fixed at $\psi = 1$ when $A_1(0) = [1, 0]$, $A_1(0) = 5/\sqrt{26}[1, i/5]$, $A_1(0) = 5/\sqrt{29}[1, 2i/5]$, $A_1(0) = 5/\sqrt{34}[1, 3i/5]$, $A_1(0) = 5/\sqrt{41}[1, 4i/5]$, and $A_1(0) = 1/\sqrt{2}[1, i]$; the transmission spectra are shown Fig. 5. It is noticed that resonant mode split occurs in given condition in the case of inputting linearly and elliptically polarized light and the positions of resonant peaks are identical. In other words, regardless of the phase relationship between x-direction and y-direction components, resonant mode split occurs and the positions of resonant peaks are identical. The

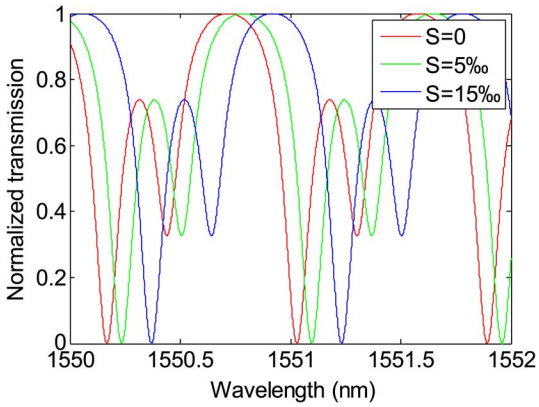


Fig. 6. Normalized transmission spectra at three different salinity when inputting elliptically polarized light and $\psi = 1$.

partially polarized light, which can also be decomposed into x-direction and y-direction components with uncertain phase relationship, can be regarded as a random collection of linearly, elliptically and circularly polarized light. Different proportions of linearly, elliptically and circularly polarized light result in different extinction ratios; however, the positions of resonant peaks are the same. That is to say, when inputting partially polarized light, the increase of $|\psi|$ also result in resonant mode split; the positions of resonant peaks are identical with those in the case of inputting linearly or elliptically polarized light. Thus, it is effective to analyze the positions of resonant peaks by inputting linearly or elliptically polarized light.

### 2.4. Response of Split Modes to Salinity

To investigate the response of split modes to salinity, a salinity sensing model is established. The eigenvalue equation for fundamental mode is given by [19]

$$\left\{\frac{J_1'(U)}{UJ_1(U)}+\frac{K_1'(W)}{WK_1(W)}\right\}\left\{\frac{J_1'(U)}{UJ_1(U)}+\frac{n_2^2K_1'(W)}{n_1^2WK_1(W)}\right\}=\left(\frac{\beta}{kn_1}\right)^2\left(\frac{V}{UW}\right)^4 \tag{6}$$

where $n_1$ is the refractive index (RI) of fiber, $n_2$ is the RI of NaCl solution, $k = 2\pi/\lambda$, $\beta$ is the propagation constant, $d$ is the diameter of fiber, $U = d(k^2n_1^2 - \beta^2)^{1/2}/2$, $W = d(\beta^2 - k^2n_2^2)^{1/2}/2$, $V = d(k^2n_1^2 - k^2n_2^2)^{1/2}/2$, $J_1$ is the Bessel function of the first kind, and $K_1$ is the modified Bessel function of the second kind. When $\psi = 1$ and $A_1(0) = 10/\sqrt{101}[1, i/10]$, the transmission spectra at salinity of 0, 5‰, and 15‰ are shown Fig. 6. It shows that the split modes have the same free spectrum range (FSR), and the resonant peaks get equal red-shift with the increasing salinity. This indicates that the split modes have the same characteristics except extinction ratio, and the response of split modes to salinity changing are the same.

## 3. Salinity Sensing Experiment

It is noticed that an evident resonant mode splitting can be observed only when $|\psi|$ is large enough, for example, $|\psi| > 0.2$ should be met in the model mentioned above. When MKRs immersed in solution, due to the tension in liquid, the deviation angle value $|\psi|$ of knot area is relatively large and meet the resonant mode split condition.

The schematic diagram of the experimental system is shown in Fig. 7(a). The system consists of supercontinuum source, optical spectrum analyzer, MKR and sample cell. Supercontinuum source provides broadband partially polarized light and a salinity meter is used to measure salinity.

In experiment, a 750-$\mu$m-diameter MKR [shown in Fig. 7(b)] with 200-$\mu$m-length twisted coupler is assembled from a 3.5-$\mu$m-diameter silica microfiber. The spectra at different salinity are shown in Fig. 8. The FSR resonant mode 1 and 2 are, respectively, 0.700 nm and 0.696 nm, and

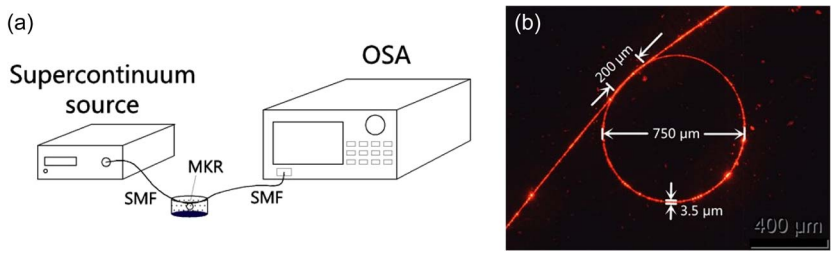


Fig. 7. (a) Schematic diagram of experimental system. (b) Optical microscope image of the 750-$\mu$m-diameter MKR with 200-$\mu$m-length twisted coupler.

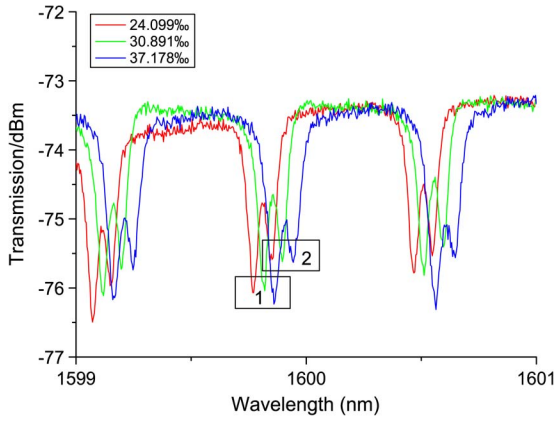


Fig. 8. Experimental spectra of MKR.

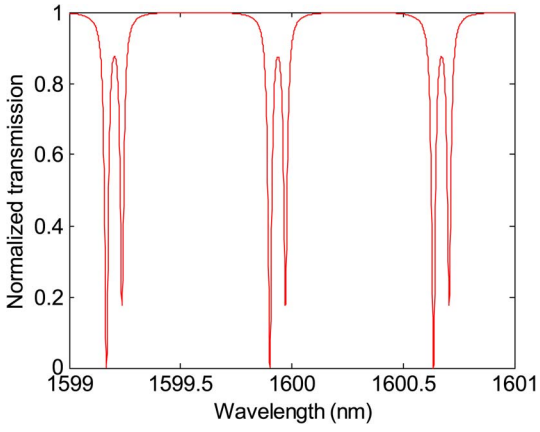


Fig. 9. Theoretical normalized transmission spectrum of MKR.

their spacing is 0.072 nm. Furthermore, the resonant peaks get approximately equal shift toward the long wavelength with the increasing salinity. Results shown here are consistent with theory.

The deviation angle, which is hard to measure in experiment, can be estimated by theoretical calculation. Based on the experimental parameters of MKR, the iteration computing is performed. When $A_1(0) = 20/\sqrt{401}[1, i/20]$, $\psi = 0.3$ or $A_1(0) = 20/\sqrt{401}[1/20, i]$, and $\psi = -0.3$, the spectrum is shown in Fig. 9. The FSR of two resonant modes are 0.734 nm and the spacing between them is 0.072 nm, which is in good agreement with the measured values. It indicates that the experimental deviation angle is about $\pm 0.3$.

## 4. Conclusion

In conclusion, resonant mode split and its characteristics are studied in this paper. The relationship between deviation angle $\psi$ of knot area and resonant mode split is investigated theoretically. In the case of inputting linearly or elliptically polarized light, $|\psi|$ increasing large enough result in resonant mode split. On this basis, the resonant mode split in the case of inputting partially polarized light is also studied. In this case, the positions of resonant peaks are identical with those in the case of inputting linearly or elliptically polarized light. It shows that resonant mode split may be appeared in various sensing as long as $|\psi|$ is large enough.

Salinity sensing model based on MKR is also established, which takes elliptically polarized light as input. Results show that resonant mode split occurs at different salinity and the split modes have the same FSR and response to salinity changing.

Salinity sensing experiment is finally performed to obtain the transmission spectra with split modes. The split modes have the same FSR and response to salinity changing, which is consistent with theoretic results. In most sensing experiment, only the shifts of resonant peaks are concerned. The split modes have almost the same characteristics, exclusive of extinction ratio and thus one of resonant modes can be analyzed. The analysis on resonant modes presented here may offer useful references for sensing applications.

## References


[1] R. C. Jorgenson and S. S. Yee, "A fiber-optic chemical sensor based on surface plasmon resonance," *Sens. Actuators B, Chem.*, vol. 12, no. 3, pp. 213–220, Apr. 1993.

[2] A. Hassani and M. Skorobogatiy, "Design of the microstructured optical fiber-based surface plasmon resonance sensors with enhanced microfluidics," *Opt. Express*, vol. 14, no. 24, pp. 11 616–11 621, Nov. 2006.

[3] J. Albert, S. Lepinay, C. Caucheteur, and M. C. DeRosa, "High resolution grating-assisted surface plasmon resonance fiber optic aptasensor," *Methods*, vol. 63, no. 3, pp. 239–254, Oct. 2013.

[4] Z. Zhang *et al.*, "On-fiber plasmonic interferometer for multi-parameter sensing," *Opt. Express*, vol. 23, no. 8, pp. 10 732–10 740, Apr. 2015.

[5] K. S. Lim *et al.*, "Resonance condition of a microfiber knot resonator immersed in liquids," *Appl. Opt.*, vol. 50, no. 30, pp. 5912–5916, Oct. 2011.

[6] X. Li and H. Ding, "A stable evanescent field based microfiber knot resonator refractive index sensor," *IEEE Photon. Technol. Lett.*, vol. 26, no. 16, pp. 1625–1628, Aug. 2014.

[7] Y. Wu, Y. Rao, Y. Chen, and Y. Gong, "Miniature fiber-optic temperature sensors based on silica/polymer microfiber knot resonator," *Opt. Express*, vol. 17, no. 20, pp. 18 142–18 147, Sep. 2009.

[8] H. Yang, S. Wang, X. Wang, Y. Liao, and J. Wang, "Temperature sensing in seawater based on microfiber knot resonator," *Sensors*, vol. 14, no. 10, pp. 18 515–18 525, Oct. 2014.

[9] Y. Wu, T. Zhang, Y. Rao, and Y. Gong, "Miniature interferometric humidity sensors based on silica/polymer microfiber knot resonators," *Sens. Actuators B, Chem.*, vol. 155, no. 1, pp. 258–263, Jul. 2011.

[10] M. A. Gouveia, P. E. S. Pellegrini, J. S. dos Santos, I. M. Raimundo, and C. M. B. Cordeiro, "Analysis of immersed silica optical microfiber knot resonator and its application as a moisture sensor," *Appl. Opt.*, vol. 53, no. 31, pp. 7454–7461, Nov. 2014.

[11] K. S. Lim *et al.*, "Current sensor based on microfiber knot resonator," *Sens. Actuators A, Phys.*, vol. 167, no. 1, pp. 60–62, May 2011.

[12] X. Li, and H. Ding, "All-fiber magnetic-field sensor based on microfiber knot resonator and magnetic fluid," *Opt. Lett.*, vol. 37, no. 24, pp. 5187–5189, Dec. 2012.

[13] O. Schwelb, "Transmission, group delay, and dispersion in single-ring optical resonators and add/drop filters—A tutorial overview," *J. Lightw. Technol.*, vol. 22, no. 5, pp. 1380–1394, May 2004.

[14] M. Sumetsky, Y. Dulashko, J. M. Fini, A. Hale, and D. J. DiGiovanni, "The microfiber loop resonator: Theory, experiment, and application," *J. Lightw. Technol.*, vol. 24, no. 1, pp. 242–250, Jan. 2006.

[15] G. Wang, P. P. Shum, L. Tong, C. M. Li, and C. Lin, "Polarization effects in microfiber loop and knot resonators," *IEEE Photon. Technol. Lett.*, vol. 22, no. 8, pp. 586–588, Apr. 2010.

[16] Q. Li, T. Wang, Y. Su, M. Yan, and M. Qiu, "Coupled mode theory analysis of mode-splitting in coupled cavity system," *Opt. Express*, vol. 18, no. 8, pp. 8367–8382, Apr. 2010.

[17] J. Yu *et al.*, "Theoretical analysis of resonant mode splitting in a single microfiber knot-ring resonator," in *Proc. 13th Int. Conf. NUSOD*, 2013, pp. 121–122.

[18] K. Morishita and T. Yamaguchi, "Wavelength tunability and polarization characteristics of twisted polarization beamsplitting single-mode fiber couplers," *J. Lightw. Technol.*, vol. 19, no. 5, pp. 732–738, May 2001.

[19] L. Tong, J. Lou, and E. Mazur, "Single-mode guiding properties of subwavelength-diameter silica and silicon wire waveguides," *Opt. Express*, vol. 12, no. 6, pp. 1025–1035, Mar. 2004.

[20] S. Wang, J. Wang, G. Li, and L. Tong, "Modeling optical microfiber loops for seawater sensing," *Appl. Opt.*, vol. 51, no. 15, pp. 3017–3023, May 2012.